COMPARISON OF PREDICTED PERFORMANCE OF VERTICAL AXIS WIND TURBINE USING OVERSET MESH AND SLIDING MESH

Sandeep Yadav [1], Srinivas V Veeravalli [2*], Sidh Nath Singh [2*]

1 PhD Student, Department of Applied Mechanics, Indian Institute of Technology Delhi, New Delhi India-110016

2 Professor, Department of Applied Mechanics, Indian Institute of Technology Delhi, New Delhi, India (Corresponding Author)

ABSTRACT

The flow behaviour of Vertical Axis Wind Turbine (VAWT) is highly unsteady even at a constant rotor speed and fixed free-stream velocity and therefore predicting the aerodynamic performance accurately is a computational challenge. Our study aims at presenting the comparison of two different mesh strategies (i) Sliding Mesh and (ii) Overset Mesh. Assuming the flow to be 2D, a computational study has been carried out using the commercially available ANSYS Fluent CFD (URANS) code. After ensuring grid independence and numerical stability, simulations are carried out at a fixed wind speed of 9 m/s and a tip speed ratio of 2.33. The turbine configuration chosen is three-bladed H-rotor vertical axis wind turbine having airfoil section NACA0021 and solidity ratio of 0.25 based on the diameter of the turbine. The power coefficient (C_P) values obtained from both techniques are compared with the numerical and experimental measurements of Castelli et al. (2011). It is found that at TSR 2.33, the C_P for overset mesh is predicted as 0.365 whereas, for the sliding mesh, it is 0.43. The results are in better agreement with the experimental results using the overset grid approach as compared to the sliding mesh approach. This comparison and ease of mesh generation using the overset grid approach will be helpful in analyzing the dual rotor VAWT (D-VAWT) configuration or any other innovative complex configuration which could improve the aerodynamic efficiency of VAWT.

Keywords: VAWT, Darrieus, H-rotor, Overset/Chimera Mesh, Vertical Axis Wind Turbine, CFD

NONMENCLATURE

C_P	Averaged Power Coefficient [-]

y+	Dimensionless wall distance [-]
Re	Reynolds Number [-]
C_d	Drag Coefficient [-]
C_l	Lift Coefficient [-]
C_m	Moment Coefficient
c	Chord [m]
Δt	Time step size [s]
TSR	Tip Speed Ratio[-]
V∞	Free-stream Wind Speed[m/s]
n	Number of blades
N	Revolutions per minute
θ	Azimuthal increment[˚degrees]
ω	Angular velocity [rad/s]

1. BACKGROUND AND INTRODUCTION

With the increasing population and their dependency on the power supply, the demand for electricity has been increasing over the years. At the same time, the pace of depletion of fossil fuel reserves and environmental issues related to fossil fuels has forced the researchers to find feasible and sustainable alternatives for generation of electricity to meet the growing demands. The renewable energy seems to be the best sustained alternative. The common renewable energy sources are Solar, Hydro and Wind Energy.

Among all the renewable resources, globally wind energy is growing relatively at faster pace. Also, harvesting wind energy at domestic levels as well as at large scale has become quite feasible and affordable with the advent of Vertical Axis Wind Turbines because of small land requirements for installation and low maintenance. Though the performance of vertical wind turbines is not at par with that of HAWTs but their

insensitivity to the flow direction and easy maintenance makes them the topic of research[1].

The flow behavior inside and around the VAWT is inherently unsteady even for the fixed freestream velocity. The reasons behind the unsteadiness are (i) deflection of flow by the blade motion which in turn generates the pressure difference in the vicinity, (ii) interaction of freestream and pressure waves, (iii) wake and pressure wave interaction with downstream rotor blades. To understand and capture the flow unsteadiness is a challenging task. Many analytical models have been developed to understand the aerodynamic performance of VAWT[2]–[4]. The primary limitation is non-availability of precise experimental data for aerodynamic coefficients of airfoils.

CFD models have a crucial role in analyzing and predicting the aerodynamic behavior of Vertical Axis Wind Turbines. The accurate prediction of aerodynamic performance in CFD mainly depends on the turbulence modelling, computational grid strategy and the proper boundary conditions. In literature, mostly the VAWT CFD simulations have been carried out using the sliding mesh strategy[5]–[7] whereas very few reported using the overset grid approach [8], [9]. In 2011, Castelli et al.[6] conducted two-dimensional simulations and experiments on a straight bladed rotor having NACA0021 airfoil profile. He compared the experimental and numerical power coefficient values over a range of tip speed ratios and reported the overestimation of the numerical results using the sliding mesh technique. In 2018, Naccache and Paraschivoiu [10] performed a URANS CFD study on D-VAWT (Dual VAWT) using the combination of sliding mesh and dynamic mesh technique. The combination of techniques was used in order to define the path of motion. This study could be done by employing overset grid approach which would have simplified the mesh generation and complex motion path inducing minimal numerical errors.

This paper mainly presents the comparison of coefficient of power predicted by the CFD simulations using the two different advanced computational grid techniques i.e. Sliding mesh and Overset mesh. In 1986, M Rai[11] explained the treatment of zonal boundaries for Euler equation calculations i.e. a basis for sliding mesh technique and Steger et al.[12] discussed over the application of overset grid scheme.

2. COMPUTATIONAL METHODOLOGY

This section mainly describes the methodology used in terms of (i) geometry, (ii) computational domain, grid generation approach and (iii) boundary conditions and solver settings.

2.1 Geometry

The geometry of H-rotor (Fig. 1) used for carrying out the CFD simulations was same as that of Castelli et al.[6] The VAWT model features are provided in the Table 1
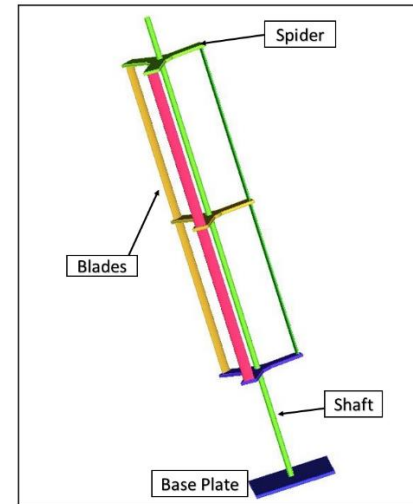

Fig. 1. Schematic of H-rotor

Parameter	Value
Blade Profile	NACA0021
No. of Blades	3
Chord Length	85.8 mm
Diameter	1030 mm
Height	1456.4 mm
Solidity Ratio	0.25
Swept Area	1.236 m^2

Table 1. VAWT Model Main Features

2.2 Computational Domain

The selection of the computational domain for solving the discretized equations is an important step in CFD and needs a lot of effort. The rectangular computational domain is taken as 60 rotor diameters downwind of rotor and 38 diameters upwind as shown in Figure 2
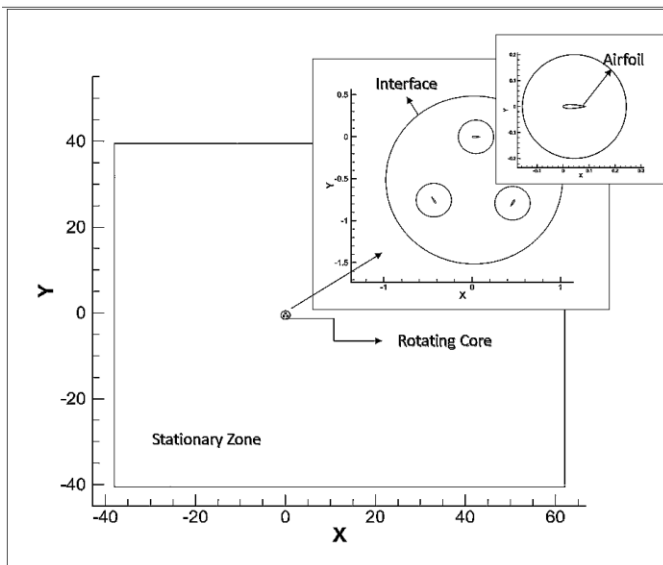
Fig. 2. Schematic of Computational Domain (Dimensions are in m)

Fig. 4. Sliding Mesh

2.3 Mesh Generation Approach

The paper reports the 2D CFD simulation of VAWT using the two mesh strategies. Figure 3 shows the highlights of Overset mesh and Figure 4 shows the sliding mesh. Both the techniques are based on moving mesh. The Overset mesh is also known as overlapping mesh or Chimera mesh because it uses chimera interpolation. This mesh is used for the simulation which involves complex relative motion between the parts and it provides greater flexibility in generating mesh for complex regions of interest. In this technique, there is one background mesh and a mesh containing the moving part which is superimposed on the background mesh and the data is interpolated between the two.
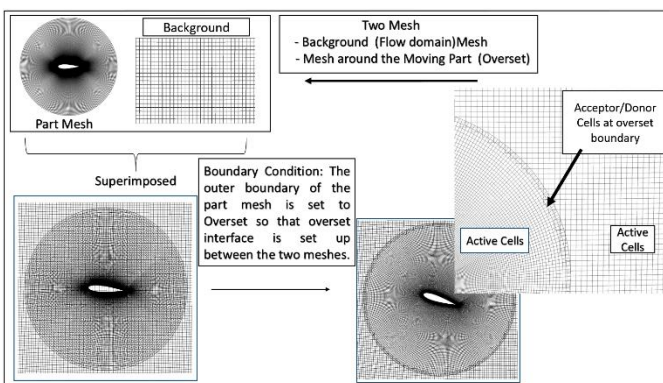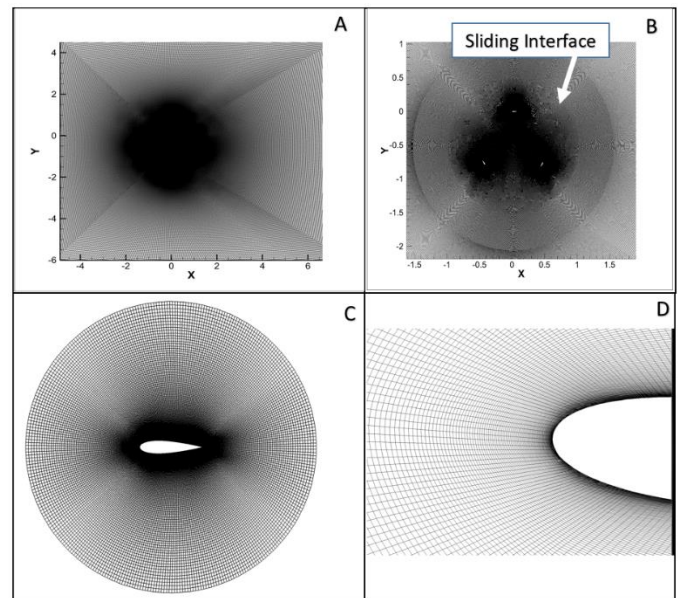

Fig. 3. Overset Mesh Strategy

The interpolation is done by sorting out the cells. It sorts the cells in four categories i.e. Active, Passive, Acceptor and Donor cells. The active cells are those where discretized equations are solved and passive cells are basically dead cells where no equations are solved. Acceptor and the donor cells are the links between the meshes at boundaries. The strategy for this type of moving mesh technique is depicted in Figure 3. The sliding mesh is a special case of dynamic meshing. Sliding mesh uses two or more mesh zones so that an interface is created between the two mesh zones. The non-conformed mesh zones have relative motion between them and the information is interpolated through the computation of fluxes. The mesh plays a crucial role in capturing the required flow characteristics and rate of convergence. These factors depends solely on the type of grid, the size and number of cells. Although there is no such specific theory for the grid generation approach as it changes with the type of problem we are dealing with. So, following one approach may or may not suit well for a particular problem. Besides the mesh, the flow depends on the characteristics of the turbulence model for the problem. The sizing of the grid also changes according to the presence of wall regions. The quality of grid such as skewness, orthogonality, aspect ratio etc. could be easily checked using grid generation tools which helps in creating the right grid for the fast convergence. The SST k−ω turbulence model with curvature correction[13] is employed for the present study as it behaves well for the adverse pressure gradients and separated flows. For resolving the viscous sub layer, the first layer thickness near the wall is kept as .027 mm (y+

= 1) and sizing increment of 1.005 geometric ratio is applied to take care of smooth increment of cell size. Structured quadrilateral mesh with appropriate inflation layer is made around the airfoils. The mesh and refinement regions highlight can be seen from the Figure 3 and 4. After the grid independence study, the final mesh size of 1.1 million cells was adopted for the study.

2.4 Boundary Conditions and Solver Settings

The Finite Volume Method (ANSYS Fluent CFD code) has been used as the solver for the study. The development of boundary layer on the airfoils of turbine strongly depicts its performance. Hence, the two equation SST k−ω model with curvature correction is selected as closure equation set for URANS. The boundary conditions are given in the Table 2. To reduce the spatial discretization error, second order upwind scheme has been applied for discretization of momentum, turbulent kinetic energy and specific dissipation rate. Least squares cell based method is selected for the discretization of spatial gradients. For the pressure velocity coupling, COUPLED scheme is used for overset mesh. In this algorithm, the pressure based continuity equation and momentum equations are solved parallelly. In time marching simulations, time step is calculated on the basis of CFL condition. The time scale found, keeping the CFL number to be 1 was of order 10^{-5}. As reported in literature, time step size calculation was calculated on the basis of time taken by turbine for 1° azimuthal angle increment. So, for TSR 2.33, Δt comes out to be 4×10^{-4} seconds and is found appropriate for the simulations.

$$\Delta T = \frac{60}{N*360} \qquad (1)$$

Though choosing the smaller time step resolves turbulent scales better but, the difference was seen to be insignificant. The Table 2 describes the other boundary conditions. The inflow wind speed was kept at $U\infty$ = 9m/s with inlet turbulence intensity of 5%. The simulations are initialized with the steady RANS calculations. After achieving the steady state solution, the time marching URANS calculations are carried out until the value of scaled residuals were lower than 10^{-5}.

Name	Type
Ring- 1, 2, 3	Overset/Interface(Sliding)
Airfoil-1,2,3	Moving Wall
Inlet	Velocity-Inlet
Outlet	Pressure-Outlet
Symmetry	Symmetry

Table 2. Boundary Conditions

The time marching calculations required 25 to 30 iterations for each time step. For setting up the reference case, one simulation was carried out for 50 revolutions and found insignificant change (less than 1%) in the coefficient of moment for two consecutive revolutions after 17 revolutions of turbine. Benchmarking the simulation, for other TSR values, simulations are carried out only up to 20 revolutions. The convergence of the revolution with the flow can be seen from the Figure 5.

3. RESULTS AND DISCUSSIONS

This section mainly presents the simulation results of two types of moving mesh techniques. To compare these two techniques, it has been ensured that the mesh count for both types of mesh is as close as possible with appropriate refinement for near wall regions. The sliding mesh uses a non-conformal interface at the boundary whereas the overset mesh uses overlapping cell zones. The two meshes are made exactly the same except at the boundaries. In overset mesh, it was ensured that the overlapping cells are of the same size as that of the cells at the non- conformal interface of sliding mesh. Also, the size and shape of overset boundary cells are the same as that of the background cell over which the overset mesh moves. This enables the correct comparison of the two techniques.

The aerodynamic quantities of interest i.e. the coefficient of power and the coefficient of moment as a function of azimuthal position are computed for comparing the two mesh strategies.

The instantaneous moment coefficient is calculated from the equation (2) as:

$$C_m^{inst}(\theta) = \frac{T(\theta)}{0.5\rho A_{swept}V_\infty^2 R} \qquad (2)$$

And the power coefficient is calculated using equation (3) as: $\qquad C_p^{inst} = TSR * C_m^{inst} \qquad (3)$

Where, $\qquad TSR = \frac{R\omega}{V_\infty}$

The predicted results are compared with experimental and numerical results of Castelli et al. [6] over a range of TSR values using NACA0021 three straight bladed H-rotor. The comparison of the experimental and numerical results of the Castelli et al. [6] was significantly different with deviation being as large as 65 % at higher TSR and 186% at lower TSR (Table 3). The numerical work of Castelli et al. [6] is with the sliding mesh technique and two equation k−ε realizable turbulence model with enhanced wall treatment. The results of sliding mesh in the present study using SST k−ω turbulence model with curvature correction at two TSR values are evaluated and

compared with the numerical results. The present numerical results match very well with the numerical results reported. The deviations with experimental results remains the same. The same study has been conducted using the overset mesh for the TSR value of 2.33 using the SST k–ω turbulence model with curvature correction and results show improvement in terms of comparison with the experimental results. The comparison shows a deviation of 143% at lower TSR and for higher TSR the deviation is only 42%. These deviations are significantly lower than the deviations observed for the sliding mesh results. Hence, it can be concluded that the overset mesh gives better results than the sliding mesh.
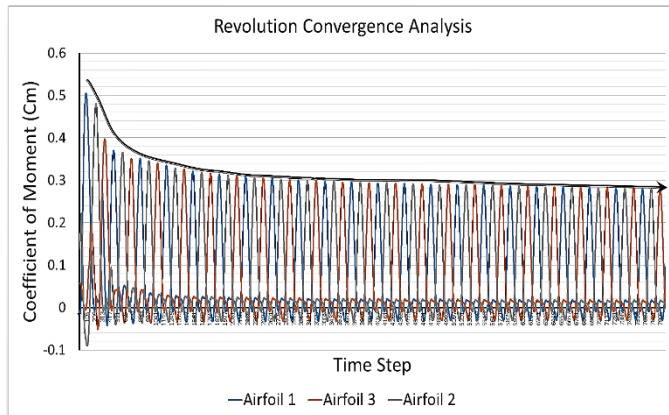

Fig. 5. Variation of C_m with the flow time

To understand the reasons for difference in predictions for the two different mesh techniques, Figure 6 and Figure 7 are plotted which show the variations in the C_m value and instantaneous C_P value with azimuthal position for both meshes respectively.
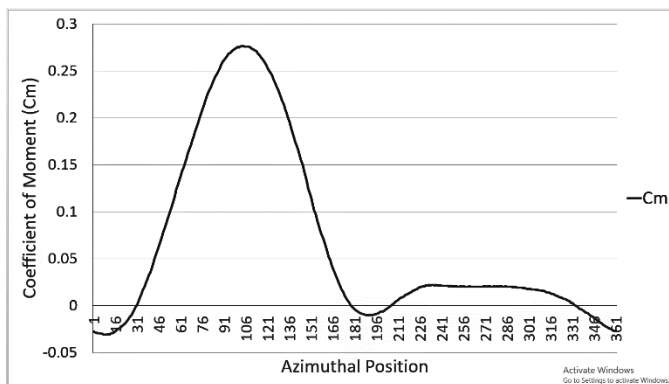

Fig. 6. Instantaneous C_m as a function of azimuthal position for single blade at TSR 2.33 using Overset Mesh
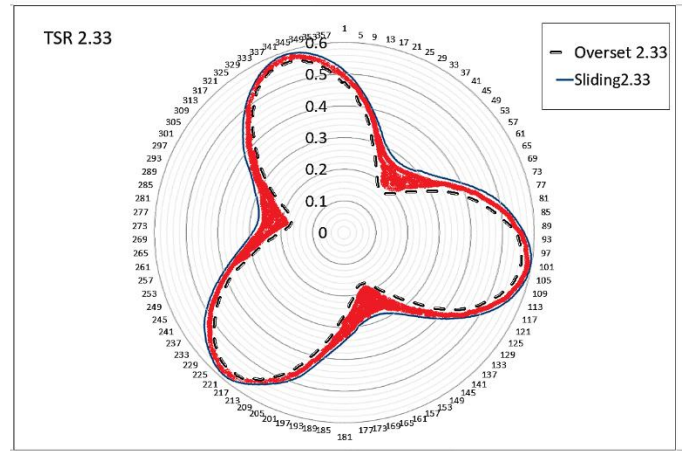

Fig. 7. Instantaneous C_P as a function of time for three blades at TSR 2.33 using Overset and Sliding Mesh

Figure 6 shows that major contribution of moment comes mainly during the upwind blade travel i.e. between the azimuthal positions of 30°-175° whereas during the downwind travel i.e. between the azimuthal positions 175° to 330°, there is a negligible contribution to the overall power. The reduction in the moment contribution in this region attributed to the interaction of the upwind blade wake with the blade in the downwind region. However, there is negative moment contribution between the azimuthal positions -30° and +30°. The maximum moment for single blade at TSR 2.33 occurs between the azimuthal positions of 90°-110°.

The distribution and variation of C_P as a function of azimuthal position for sliding mesh and overset mesh for TSR 2.33 is highlighted in Fig. 7. At TSR 2.33, the C_P value using the overset mesh is found to be 0.365 and 0.43 using the sliding mesh respectively. The experimental value is only 0.27.The comparison can also be seen from Table 3.

TSR	Experiments Castelli et al.	Numerical Castelli et al.	Sliding Mesh	Overset Mesh
2.04	0.14	0.40	0.41	0.34
2.33	0.257	0.428	0.43	0.365

Table 3. Comparison of C_P Values

The C_m and C_P variation for sliding mesh is more pronounced than for the overset mesh. The difference in the C_P curves for both type of mesh strategies is highlighted in red color. The reason behind these variation can be attributed to the numerical errors introduced due to interpolations at the sliding interface of the sliding mesh or may be the interpolations between

the acceptor cells and the donor cells of the chimera/overset mesh.

4. CONCLUSIONS

In this paper, the comparison of two numerical techniques (i) Sliding Mesh, (ii) Overset Mesh for the simulation of 2D H-rotor Vertical Axis Wind Turbine has been carried out. The C_P values predicted using the Overset mesh are better and closer to the experimental results compared to the sliding mesh. So, for simulating the flow around Vertical Axis Wind Turbine, the overset mesh performs better for performance prediction with the ease of mesh generation and refinement in the required regions. Though both the mesh techniques produce reliable CFD results, the overset mesh is found computationally expensive than the sliding mesh in terms of CPU hours. The other difficulty with the overset mesh is that the aspect ratio and the overlap area of acceptor and donor cells must be comparable to get proper convergence which becomes quite difficult to maintain during the rotation of one part over the other which could introduce the numerical errors and difficulty in ensuring the flux conservation through domains. Considering better predictions with overset grid approach, this study will be helpful in future CFD analysis and will support experiments for design optimization of complex, efficient VAWT configurations like D-VAWT having two axis where blades move on an oval shape path to enhance the aerodynamic efficiency of VAWT. For D-VAWT, performing CFD simulations using sliding mesh alone is not possible. This flexibility and reliability of overset grid approach makes it advantageous over the sliding mesh approach.

REFERENCE

[1]   D. E. Berg, "Vertical-Axis Wind Turbines-The Current Status of an Old Technology," Sandia Natl. Lab. Albuquerque, New Mex. USA, 1972.

[2]   R. E. Wilson and L. P.B.S., "Applied Aerodynamics of Wind Power Machines," no. Oregon State University, 1974.

[3]   J. H. Strickland, "The Darrieus Turbine: A Performance Prediction Model Using Multiple Streamtube Model," Sandia Natl. Lab. Albuquerque, New Mex. USA, no. SAND75-0431, 1975.

[4]   M. Islam, D. S. K. Ting, and A. Fartaj, "Aerodynamic models for Darrieus-type straight-bladed vertical axis wind turbines," Renew. Sustain. Energy Rev., vol. 12, no. 4, pp. 1087–1109, 2008.

[5]   R. Lanzafame, S. Mauro, and M. Messina, "2D CFD modeling of H-Darrieus Wind Turbines using a transition turbulence model," Energy Procedia, vol. 45, pp. 131–140, 2014.

[6]   M. Raciti Castelli, A. Englaro, and E. Benini, "The Darrieus wind turbine: Proposal for a new performance prediction model based on CFD," Energy, vol. 36, no. 8, pp. 4919–4934, 2011.

[7]   K. Rogowski, M. O. L. Hansen, and P. Lichota, "2-D CFD computations of the two-bladed Darrieus-type wind turbine," J. Appl. Fluid Mech., vol. 11, no. 4, pp. 835–845, 2018.

[8]   P. A. Kozak, D. Vallverdú, and D. Rempfer, "Modeling Vertical-Axis Wind-Turbine Performance: Blade-Element Method Versus Finite Volume Approach," J. Propuls. Power, vol. 32, no. 3, pp. 592–601, 2016.

[9]   G. Bangga, M. Solichin, A. Daman, D. Sa'Adiyah, A. Dessoky, and T. Lutz, "Aerodynamic performance of a small vertical axis wind turbine using an overset grid method," AIP Conf. Proc., vol. 1867, no. August, 2017.

[10]   G. Naccache and M. Paraschivoiu, "Parametric study of the dual vertical axis wind turbine using CFD," J. Wind Eng. Ind. Aerodyn., vol. 172, no. November 2017, pp. 244–255, 2018.

[11]   M. M. Rai, "A Conservative Treatment of Zonal Boundaries for Euler Equation Calculations," J. Comput. Phys., vol. 62, pp. 472–503, 1986.

[12]   J. L. Steger and J. A. Benek, "On the use of composite grid schemes in computational aerodynamics," Comput. Methods Appl. Mech. Eng., vol. 64, no. 1–3, pp. 301–320, 1987.

[13]   F. R. Menter, "Two-equation eddy-viscosity turbulence models for engineering applications," AIAA J., vol. 32, no. 8, pp. 1598–1605, 1994.

[14]   D. L. Shukla, A. U. Mehta, and K. V. Modi, "Dynamic overset 2D CFD numerical simulation of a small vertical axis wind turbine," Int. J. Ambient Energy, vol. 0750, 2018.